Chapter Ten

Miscellaneous investigations

Introduction

This chapter reports depolarization ratios and mean polarizabilities for a number of species for which data were required for various purposes. Argon was studied to determine the instrumental depolarization of the apparatus, and nitrogen was studied mainly as a secondary check on the accuracy of the equipment at various scattered light intensities. Cyclopropane and ammonia have been studied previously but since the ratios are low, exclusion of the vibrational Raman lines may be important, and it was decided to repeat the measurements in the present research.

Formaldehyde and acetaldehyde were studied as a part of a systematic investigation of species containing formyl and acetyl groups. The change in the mean polarizability and polarizability anisotropy was determined for the series formaldehyde, acetaldehyde and acetone as a function of the number of methyl groups attached to the carbonyl group. The depolarization ratios of 1,2,3,5- and 1,2,4,5-tetrafluorobenzene were recorded to assist the analysis of the temperature dependence of the Kerr effect [1]. Results for 1,4-dioxane are reported and compared with the properties of cyclohexane. Finally, results for trimethylboroxine are included as a first step in the study of gas-phase electric properties of species containing boron-oxygen rings. The depolarization ratios for 1,4-dioxane were recorded with Version 1 of the apparatus; all other values were recorded with Version 2.

Argon

The noble gases have histor cally been the choice for determining the sensitivity and accuracy of light scattering equipment [2-4], and argon has been used in the present research. If the pressure is low enough to avoid collision-induced anisotropy, the depolarization ratio for argon shoulc be zero ($I_v^h = 0$ in equation 1.7 for highly symmetric or atomic species). Hesling [4] studied argon with a previous version of the present equipment giving typical values of $100\rho_0 = 0.004 \pm 0.030$ and $100\rho_0 = 0.003 \pm 0.020$.

A sample of argon (> 99.999%) was obtained from CIG Ltd. Five conventional depolarization ratios were recorded giving $100\rho_0 = 0.032 \pm 0.007$, -0.006 ± 0.014, 0.011 ± 0.013, 0.009 ± 0.013 and 0.035 ± 0.017 with integration times of 500 s for the depolarized component and 250 s for the polarized component. It is evident that the observed ratios were attributable to statistical noise, and a definitive value for the instrumental depolarization of the apparatus was unattainable from these ratios. A negative value for the depolarization ratio is possible since the depolarized signal was slightly smaller than the depolarized background ($I_{h,b}^v > I_h^v$ in equation 2.1).

To avoid this problem, the depolarization ratio was obtained by recording the polarized and depolarized components as a function of the number density, and taking the gradients of the subsequent plots to be the depolarization ratio of argon (Chapter 2). Integration times for each gas density were 500 s for the depolarized component and 250 s for the polarized component. The count rates are plotted as a function of number density in Figures 10.1 and 10.2, where it is evident that the correlation for the depolarized signal was poor. The depolarization ratio was determined to be $100\rho_0 = 0.004 \pm 0.008$ from the gradients of the lines. Since the signal-to-noise ratio was low for the depolarized counts, it is extremely difficult to justify $100\rho_0 = 0.004$ as the instrumental depolarization of the apparatus. It is also expected that this value will change with realignment of the apparatus. Therefore, this value was not used as a correction factor for the other ratios determined in this research. It was assumed that if the depolarization ratio obtained for carbon dioxide was $100\rho_0 = 4.01$ then this would suffice for obtaining an accurate depolarization ratio of any other molecule.

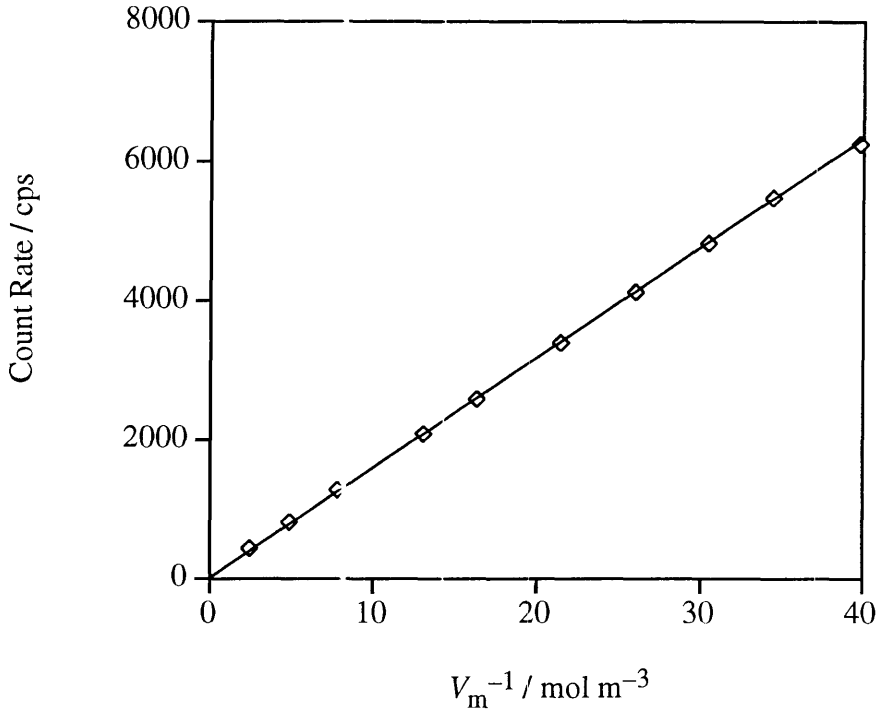

Figure 10.1 Polarized count rates for argon as a function of number density.

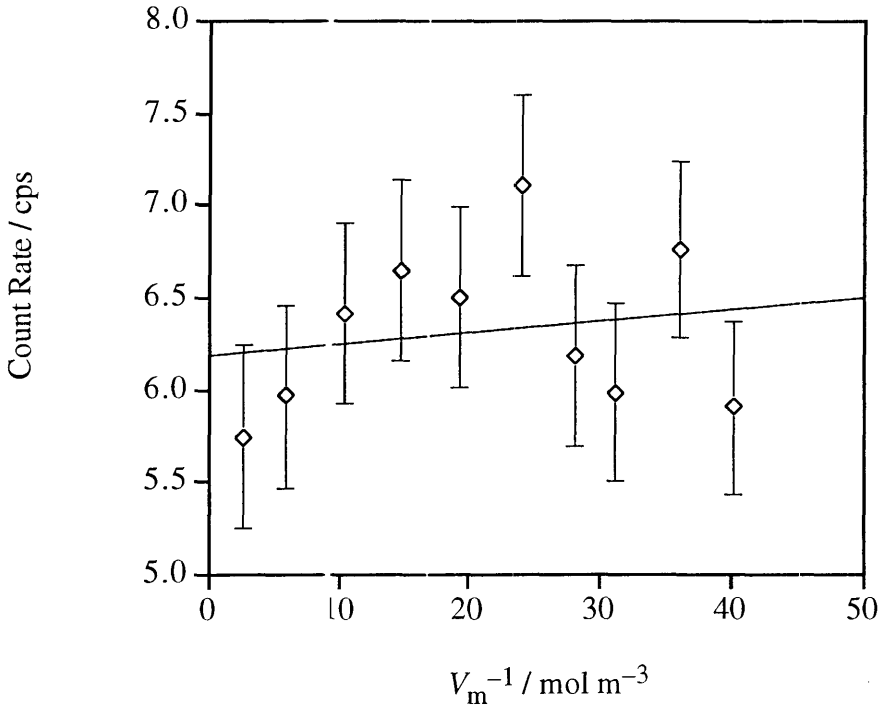

Figure 10.2 Depolarized count rates for argon as a function of number density.

Cyclopropane

A reliable depolarization ratio for cyclopropane at 632.8 nm is unavailable, although it has been reported in the form of a polarizability anisotropy [5]. The present study was undertaken to rectify this deficiency. Since the depolarization ratio is low, the vibrational Raman contribution is expected to be relatively large.

A sample of cyclopropane (> 99.9%) was obtained from CIG Ltd and used without further purification. The depolarization ratios, with inclusion and exclusion of the vibrational Raman lines, are given in Table 10.1. Integration times of 200 s for the polarized component and 400 s for the depolarized component were used. Typical polarized and depolarized count rates with inclusion of the vibrational Raman lines at 25 °C and ≈ 100 kPa were 67 490 and 111.5 cps, with background counts of 22 and 7.5 cps, respectively.

The depolarization ratios, with inclusion and exclusion of the vibrational Raman lines, were found to be $100\rho_0 = 0.154 \pm 0.002$ and $100\rho_0 = 0.123 \pm 0.002$, respectively. In comparison, for 632.8 nm, with inclusion of the vibrational Raman lines, Bridge and Buckingham [2] and Bogaard *et al.* [6] reported values of $100\rho_0 = 0.136 \pm 0.002$ and $100\rho_0 = 0.142 \pm 0.002$. A value for 488.0 nm of $100\rho_0 = 0.136 \pm 0.012$, with exclusion of the vibrational Raman lines using the R_{20} method, was reported by Monan *et al.* [7]. Clearly, there is less than satisfactory agreement between these values.

Table 10.1 Depolarization ratios for cyclopropane.

$100\rho_0$	
0.152 ± 0.003	0.123 ± 0.003[a]
0.156 ± 0.002	0.123 ± 0.002[a]
0.154 ± 0.002	0.125 ± 0.002[a]
0.154 ± 0.002	0.121 ± 0.002[a]
0.153 ± 0.002	0.122 ± 0.002[a]

[a] Vibrational Raman lines excluded.

The mean polarizability, with exclusion of the vibrational Raman lines, was found to be $\alpha = 6.55 \pm 0.02$ using density second virial coefficients from the literature [8], but this value is too high when compared with the literature values. The mean polarizability of $\alpha = 6.28 \pm 0.06$ (an uncertainty of $\pm$ 1% was assumed) reported by Bogaard *et al.* from gas-phase refractive indices was used in the analysis. This value agrees with recent measurements of refractive indices by Hohm [9,10], and semi-empirical calculations by Thomas, Mulder and Meath [11] using the Kirkwood and Unsöld procedures.

Using the depolarization ratio, with exclusion of the vibrational Raman lines, and the mean polarizability of Bogaard *et al.* gives $\Delta\alpha = -0.85 \pm 0.01$, $\alpha_{\parallel} = 5.71 \pm 0.06$ and $\alpha_{\perp} = 6.56 \pm 0.06$. The present polarizability anisotropy is slightly higher than the value given by Lukins *et al.* [5] of $\Delta\alpha = -0.818 \pm 0.042$ using the depolarization ratio reported by Monan *et al.*, but this value assumed that the polarizability anisotropy and the depolarization ratio have the same dispersion.

Böttcher *et al.* [12] have derived values for the magnetizability anisotropy and the molecular g values of cyclopropane from a study of the microwave Zeeman effect of 1,1-dideuterocyclopropane. The results are in excellent agreement with studies of the microwave Zeeman effect of the van der Waals complexes C_3H_6-HCl and C_3H_6-HCN by Aldrich *et al.* [13]. This suggests that additivity of the above properties holds to a high degree of approximation for van der Waals complexes, and this is in contrast to the conclusions drawn by Lukins *et al.* [5] from a study of the temperature dependence of the Cotton-Mouton effect of cyclopropane.

Lukins *et al.* reported a magnetizability anisotropy of $\Delta\chi = (-19.2 \pm 1.9) \times 10^{-29}$ J T^{-2}, which was recalculated using the present polarizability anisotropy to give $\Delta\chi = (-18.4 \pm 1.5) \times 10^{-29}$ J T^{-2}. This result is still higher than the values of $\Delta\chi = (-16.1 \pm 1.6) \times 10^{-29}$ J T^{-2} and $\Delta\chi = (-16.3 \pm 0.5) \times 10^{-29}$ J T^{-2} reported by Aldrich *et al.* and Böttcher *et al.*, respectively, although the uncertainties are relatively large. Furthermore, the value of Lukins *et al.* is higher than a recent result of $\Delta\chi = (-16.2 \pm 1.1) \times 10^{-29}$ J T^{-2} derived from a study of the temperature dependence of the field-gradient induced birefringence by Watson [14].

Watson and Aldrich *et al.* r:port quadrupole moments of Θ = (3.88 ± 0.23) x 10^{-40} C m^2 and Θ = (3.5 ± 1.3) x 10^{-40} C m^2, respectively. A quadrupole moment of Θ = (5.9 ± 1.6) x 10^{-40} C m^2 rec alculated by Lukins *et al.* from a single-temperature study of the field-gradient induced birefringence by Buckingham *et al.* [15] is too high. Recalculating this value again using the present polarizability anisotropy gives Θ = (5.7 ± 1.6) x 10^{-40} C m^2, which is still too high. Watson noted that the value reported by Buckingham *et al.* is too high bec ause the contribution to the field-gradient induced birefringence from the quadrupole hyperpolarizability was assumed to be negligible, whereas Watson determined the contribution to be +52% at 300 K. Quadrupole moments of Θ = 8.40 x 10^{-40} C m^2 and Θ = 8.13 x 10^{-40} C m^2 from ab initio calculations by Amos and Williams [16] and Spac cman [17] are also too high. Further computational studies of cyclopropane are required to rectify this discrepancy. It is noted that a collision-induced infrared absorptic n study of cyclopropane by Dagg *et al.* [18] tends to support the larger values of the qu adrupole moment. Dagg *et al.* asserted that a lower quadrupole moment cannot accour t for the observed collision-induced absorption, but this method is reliant on the choice c f an accurate intermolecular potential.

Formaldehyde and acetaldehyde

A method which combines Rayleigh light scattering and Kerr effect measurements with ab initio calculations to deter nine the polarizabilities of C_s or higher symmetry molecules has been developed by Ritchie *et al.* [19]. This method makes it possible to determine the polarizabilities of molecules of the type given in Figure 10.3. Therefore, the influence of functional groups such as the halogens on the formyl and acetyl groups can be determined.

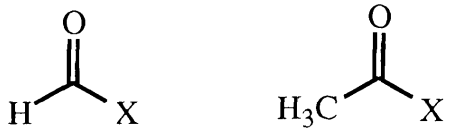

Figure 10.3 Structures containing formyl and acetyl groups of interest in the present research, where X = H, OH, F, Cl, Br, NH_2 etc.

Studies of formaldehyde and acetaldehyde were commenced as part of a systematic investigation of the above species, and research on the acetyl halides has followed [20]. Combining the results for formaldehyde and acetaldehyde with those for acetone [6] should permit a study of the change in the mean polarizability and polarizability anisotropy as a function of methyl substitution into the carbonyl group.

Formaldehyde

Formaldehyde is the smallest molecule containing a carbonyl group, and a reliable depolarization ratio is unavailable. Unfortunately, formaldehyde readily polymerizes to form dimers and trimers such as trioxane and, in the extreme, polyoxymethylene [21]. Problems were expected to occur due to the presence of polymer particles or dust within the light scattering cell.

A sample of formaldehyde, dissolved in water with methanol as a stabilizer, was obtained from the Aldrich Chemical Company. Special apparatus was constructed to allow generation of the monomer from purified paraformaldehyde. The purification of paraformaldehyde and subsequent monomer generation followed a procedure given in the literature [22], except that the glass wool was not cooled, since a greater rate of deposition of polymer was expected at the lower temperature (and still occurred in the unheated section of the apparatus). Furthermore, calcium chloride, instead of phosphorus pentoxide, was used as the drying agent, and was also successful in blocking the passage of solid polymer. It was mentioned by Walker [23] that drying agents tend to promote polymerization. The final purity of the formaldehyde gas was unknown, and determining the purity of the sample within the apparatus would be complicated by the presence of dimers, trimers and polymer fragments. The cell temperature was kept at 97.5 °C to reduce the deposition of polymer [21,23].

Integration times of 100 s for the polarized component and 200 s for the depolarized component were used. Typical polarized and depolarized count rates, with inclusion of the vibrational Raman lines, at 97.5 °C and ≈ 26 kPa were 1 214 and 22 cps, with background counts of 15 and 8 cps, respectively. The uncertainties in the ratios which included the vibrational Raman lines were unacceptably large due to the small

signal of the depolarized component. The uncertainties for the ratios which excluded the vibrational Raman lines were reduced by quadrupling the integration times. The depolarization ratios are given in Table 10.2.

From the table, it is evident that the precision of the ratios is poor. It is strongly suspected that this was due to the interference of gas-phase dimers and trimers within the scattering cell. It would be constructive to perform a study of the pressure dependence of the depolarization ratio of formaldehyde. It is also probable that, because of the chemical nature of the interaction, a study of the temperature dependence of the depolarization ratio may also yield interesting results. The mean depolarization ratios, with inclusion and exclusion of the vibrational Raman lines, were found to be $100\rho_0 = 1.41 \pm 0.14$ and $100\rho_0 = 1.23 \pm 0.09$. Although the uncertainties are large, it is evident that the vibrational Raman contribution to the depolarization ratio is significant.

Acetaldehyde

A gas-phase depolarization ratio for acetaldehyde has not been reported. A sample of acetaldehyde (> 99%) was obtained from the Aldrich Chemical Company and was used without further purification, but was subjected to two freeze-pump-thaw cycles including a vacuum distillation before entry into the light scattering cell. Integration times of 100 s for the polarized component and 200 s for the depolarized component were used. Typical polarized and depolarized counts with inclusion of the vibrational Raman lines at 25 °C and ≈ 40 kPa were 16 494 and 140 cps, with background counts of 25 and 5.4 cps, respectively; the depolarization ratios are given in Table 10.2. The mean depolarization ratios, with inclusion and exclusion of the vibrational Raman lines, were found to be $100\rho_0 = 0.815 \pm 0.004$ and $100\rho_0 = 0.77 \pm 0.03$. A mean polarizability was not recorded, due to pressure instability.

A comparison of the depolarization ratios, mean polarizabilities and polarizability anisotropies of formaldehyde, acetaldehyde and acetone can be made, and a summary is given in Table 10.3. The depolarization ratio for acetone reported by Bogaard *et al.* [6] is small and it is probable that the contribution from the vibrational Raman lines is significant. A reliable experimental mean polarizability for formaldehyde is unknown,

but Spackman [17] has estimated a mean polarizability at zero-frequency from ab initio calculations and solution-phase refractive indices; this value may have an uncertainty of up to 10%. Recent calculations by Sauer and Oddershede [24] at the MP2 level of theory gave zero-frequency values of α = 2.906 and $\Delta\alpha$ = 1.306 for formaldehyde, although their basis sets were not optimized for polarizability calculations.

Table 10.2 Depolarization ratios for formaldehyde and acetaldehyde.

$100\rho_0$			
formaldehyde		acetaldehyde	
1.54 ± 0.16	1.51 ± 0.11	0.815 ± 0.008	0.727 ± 0.009[a]
1.22 ± 0.13	1.16 ± 0.08[a]	0.810 ± 0.009	0.759 ± 0.010[a]
1.26 ± 0.18	1.15 ± 0.07[a]	0.818 ± 0.009	0.779 ± 0.011[a]
1.50 ± 0.16	1.27 ± 0.05[a]	0.817 ± 0.009	0.782 ± 0.011[a]
1.53 ± 0.17	1.32 ± 0.04[a]	0.779 ± 0.010[a]	0.780 ± 0.012[a]
1.34 ± 0.16			

[a] Vibrational Raman lines excluded.

Table 10.3 Depolarization ratios, mean polarizabilities and polarizability anisotropies for formaldehyde, acetaldehyde and acetone.

	$100\rho_0$	α	$\Delta\alpha$[a]
formaldehyde	1.41 ± 0.14[b]	2.93[c]	1.36
acetaldehyde	0.815 ± 0.004[b]	5.15[d]	1.81
acetone	0.530 ± 0.005[e]	7.14[e]	2.02

[a] $\Delta\alpha$ is reported as $|3\alpha\kappa|$.

[b] Present research, vibrational Raman lines included.

[c] Zero-frequency estimate based on refractivity data and ab initio calculations [17]; the uncertainty may be as high as 10%.

[d] Reference [25].

[e] Reference [6].

It is evident that the depolarization ratios decrease as the number of methyl groups attached to the carbonyl group increase, and it is probable that the mean polarizability increases more or less linearly as a function of methyl substitution. Therefore, a better value of the mean polarizability of formaldehyde at 632.8 nm would be $\alpha \approx 3.14$, which gives a polarizability anisotropy of $\Delta\alpha \approx 1.46$ (or $\Delta\alpha \approx 1.36$ if the vibrational Raman lines are excluded). The polarizabi ity anisotropies given in Table 10.3 are by no means definitive, but indicate the general variation in the electronic charge distributions within this series of molecules.

Ammonia

Despite the large amount of experimental [1,26-30] and computational [17,31-36] research devoted to the electric and magnetic properties of ammonia, the depolarization ratio has been determined only by Bridge and Buckingham [2]. Ritchie *et al.* [37] attempted a measurement of the depolarization ratio of ammonia with a previous version of the present apparatus using a 10 mW He/Ne laser, but the depolarized component of the scattered light could not be isolated from the statistical noise. It was decided to attempt such measurements again, on the assumption that the 35 mW He/Ne laser would provide a more readily observable signal.

A sample of ammonia (> 99.99%) was obtained from Matheson Gas Products and used without further purification. Integration times of 500 s for the polarized component and 1 000 s for the depolarized component were used. Typical polarized and depolarized count rates, with inclusion of the vibrational Raman lines, at 25 °C and ≈ 100 kPa were 15 000 and 32 cps, with background counts of 22 and 8 cps, respectively. The depolarization ratios, with inclusion and exclusion of the vibrational Raman lines, are given in Table 10.4. The depolarization ratio of $100\rho_0 = 0.108 \pm 0.004$ for 632.8 nm reported by Bridge and Buckingham is in good agreement with the value of $100\rho_0 = 0.091 \pm 0.009$ obtained in the present research, where both ratios have the vibrational Raman lines excluded. From the present results, the vibrational Raman contribution to the total depolarization ratio was ≈ 40%.

Only one mean polarizabili y was determined with exclusion of the vibrational Raman lines, giving $\alpha = 2.49 \pm 0.02$. Density second virial coefficients required for the conversion of pressures to number densities were obtained from the literature [8]. This value is in excellent agreement with a value of $\alpha = 2.46$ obtained from dipole oscillator-strength distributions by Meath and co-workers [26], interferometric measurements of the refractive indices by Hohm [9,10], and a mean polarizability of $\alpha = 2.47$ derived from other refractive indices [25]. The polarizability components and polarizability anisotropy were found to be $\alpha_{\parallel} = 2.68 \pm 0.03$, $\alpha_{\perp} = 2.39 \pm 0.03$ and $\Delta\alpha = 0.29 \pm 0.02$.

Table 10.4 Depolarization ratios for ammonia.

$100\rho_0$	
0.159 ± 0.008	0.090 ± 0.009^a
0.156 ± 0.007	0.102 ± 0.011^a
0.140 ± 0.008	0.092 ± 0.011^a
0.154 ± 0.009	0.081 ± 0.009^a

[a] Vibrational Raman lines excluded.

Much theoretical work on the polarizability components of ammonia has been reported in the last twenty years [17 31,33-36], with zero-frequency mean polarizabilities and polarizability anisotropies ranging from $\alpha = 2.1$ to 2.5 and $\Delta\alpha = 0.26$ to 0.39, depending on the basis set and level of theory used. The most recent published values are $\alpha = 2.371$ and $\Delta\alpha = 0.33$ reported by Sekino and Bartlett [38] using the CCSD(T) level of theory. These are slightly higher than the values reported by Maroulis [32] of $\alpha = 2.309$ and $\Delta\alpha = 0.26$ using the SDQ-MP4 level of theory, which are comparable with an earlier full MP4 calculation reported by Diercksen and Sadlej [34]. Russell and Spackman [39] have estimated the zero-point vibrational average corrections to the mean polarizability and polarizability anisotropy to be $\approx +4\%$ and $\approx -10\%$. Other computational studies have been reported [24,31,33,35,36,40,41].

Nitrogen

The depolarization ratio of nitrogen has been determined by a number of researchers, and there is general agreement that the ratio for 632.8 nm is between $100\rho_0$ = 1.00 and 1.04 when the vibrational Raman lines are included. The depolarization ratio of nitrogen was recorded during the present research as a check on the behaviour of the apparatus with respect to differing scattered light intensities. The depolarization ratio with exclusion of the vibrational Raman lines has been measured by Murphy [42] using the R_{20} method, and by Haverkort *et al* [43], but these values are for a wavelength of 514.5 nm. Therefore, part of the aim of the research was to determine the depolarization ratio of nitrogen for 632.8 nm with exclusion of the vibrational Raman lines.

A sample of nitrogen was obtained from CIG Ltd (> 99.999%) and used without further purification. Integration times ranged from 100 to 500 s for the polarized component and from 200 to 1 000 s for the depolarized component. Typical polarized and depolarized counts with inclusion of the vibrational Raman lines at 25 °C and ≈ 100 kPa were 9 757 and 108 cps, with background counts of 20 and 7 cps, respectively. The depolarization ratios obtained in the present research are given in Table 10.5. The mean depolarization ratios are reported in Table 10.6, and literature values are included.

The uncertainties in the present ratios are considerably larger than those quoted by Bogaard *et al.* [6] and Bridge and Buckingham [2]. The present ratio of $100\rho_0$ = 1.044 ± 0.024, with inclusion of the vibrational Raman lines, agrees with the literature values, especially the value of Bogaard *et al*. The ratio of $100\rho_0$ = 0.97 ± 0.03, with exclusion of the vibrational Raman lines, agrees with the value for 514.5 nm reported by Murphy, but his ratio has a large uncertainty and dispersion will lower the value.

One mean polarizability for nitrogen was measured, with exclusion of the vibrational Raman lines, giving a value of α = 1.964 ± 0.002. This value is in excellent agreement with values of α = 1.967 interpolated from refractive indices [2,6], α = 1.962 derived from dipole oscillator-strength distributions [26,27] and α = 1.975 interpolated from interferometric measurements of the refractive indices [44]. Combining the depolarization ratio, with exclusion of the vibrational Raman lines, and the mean

polarizability gives a polarizability anisotropy of $\Delta\alpha = 0.75 \pm 0.02$, and polarizability components of $\alpha_{\parallel} = 2.47 \pm 0.03$ and $\alpha_{\perp} = 1.71 \pm 0.02$. These components are in excellent agreement with recent values calculated using multireference configuration interaction theory by Spelsberg and Meyer [45], and MP2 vibrationally averaged property calculations reported by Bishop and Cybulski [46].

Table 10.5 Depolarization ratios for nitrogen.

$100\rho_0$		
1.004 ± 0.031	1.042 ± 0.027	0.939 ± 0.035[a]
1.072 ± 0.022	1.055 ± 0.021	0.953 ± 0.016[a]
1.055 ± 0.031	1.044 ± 0.013	1.011 ± 0.018[a]
1.075 ± 0.030	1.042 ± 0.014	0.980 ± 0.016[a]
1.012 ± 0.033		

[a] Vibrational Raman lines excluded.

Table 10.6 Comparison of the known depolarization ratios for nitrogen.

λ(nm)	$100\rho_0$	Reference
632.8	1.044 ± 0.024	Present work
	0.97 ± 0.03[a]	Present work
	1.042 ± 0.006	Bogaard *et al.* [6]
	1.018 ± 0.005	Bridge and Buckingham [2]
	1.02 ± 0.01	Alms *et al.* [3]
	1.00 ± 0.03	Baas and van den Hout [47]
514.5	1.04 ± 0.02[a]	Haverkort *et al.* [43]
	1.01 ± 0.03	Baas and van den Hout [47]
	0.96 ± 0.14[a]	Murphy [42]

[a] Vibrational Raman lines excluded.

A summary of the known values of the quadrupole moment of nitrogen is given in Table 10.7, and is similar to a table given by Watson [14]. The quadrupole moments derived from single-temperature measurements of the field-gradient induced birefringence have been recalculated using the present polarizability anisotropy of $\Delta\alpha = 0.75 \pm 0.02$ and also corrected by -10% to account for the contribution from the quadrupole hyperpolarizability as determined by Watson. The quadrupole moment reported by Watson was also recalculated using the present polarizability anisotropy.

The quadrupole moment by Graham, Imrie and Raab [48] from an unpublished single-temperature measurement of the field-gradient induced birefringence is in excellent agreement with the value reported by Watson, but other single-temperature measurements are considerably smaller [15,49-51]. The quadrupole moments determined by other methods [52-55], such as collision-induced far infrared absorption and the density second virial coefficient method, agree with the quadrupole moment reported by Watson. The most recent ab initio calculation reported by Bishop and Cybulski [46] includes a vibrational average of the quadrupole moment, although at the MP2 level of theory the correction for the vibrational average is negligible; this observation has been confirmed by Russell and Spackman [39].

Kling and Hüttner [56] reported a value of $\Delta\alpha\Delta\chi = (-11.5 \pm 0.4) \times 10^{-69}$ $C^2\,m^2\,T^{-2}$ from a study of the temperature dependence of the Cotton-Mouton effect. If this is combined with the polarizability anisotropy reported by Bogaard *et al.*, then a quadrupole moment of $\Theta = (-4.3 \pm 1.3) \times 10^{-40}$ C m^2 is obtained using equation 1.36, but using the present polarizability anisotropy gives a quadrupole moment of $\Theta = (-2.6 \pm 1.6) \times 10^{-40}$ C m^2 (where the rotational g value is assumed to be reliable). Equation 1.36 is dependent on the difference between two large and oppositely signed values which, in the case of nitrogen, magnifies small differences in $\Delta\chi$ values into large differences in Θ values, and large uncertainties are also a result. Further work on nitrogen is required and another study of the Cotton-Mouton effect may be beneficial.

Table 10.7 Comparison of values of the quadrupole moment for nitrogen.

Year	Method	$10^{40}\ \Theta$ / C m^2	Reference
1968	field-gradient induced birefringence, single-temperature	−4.39 ± 0.37	[50]
1977	ion-molecule scattering	−5.00 ± 1.7	[55]
1981	collision-induced far infrared absorption	−5.00 ± 0.33	[53]
1983	field-gradient induced birefringence, single-temperature	−4.60 ± 0.37	[15]
1985	collision-induced far infrared absorption	−5.04	[54]
1989	field-gradient induced birefringence, single-temperature	−4.43 ± 0.33	[51]
1991	density second virial coefficient	−4.90 ± 0.23	[52]
1993	field-gradient induced birefringence, single-temperature	−4.93 ± 0.23	[48]
1994	field-gradient induced birefringence, temperature dependence	−5.11 ± 0.20	[14]

In summary, the depolarization ratio for nitrogen, with inclusion of the vibrational Raman lines, is in good agreement with the literature values. The depolarization ratio, with exclusion of the vibrational Raman lines, was measured for 632.8 nm and the vibrational Raman contribution was found to be ≈ 7.6%. In consequence, the polarizability anisotropy was ≈ 4% lower than the value given by Bogaard *et al.* and this increased the quadrupole moment reported by Watson by 4%. Other known values of the quadrupole moment were recalculated using the present polarizability anisotropy.

1,4-dioxane

A study of 1,4-dioxane was undertaken to compare the results with the properties of cyclohexane. A sample of 1,4-dioxane was obtained from the Ajax Chemical Company. Purification followed a procedure given in the literature [22], giving a purity of > 99.9% as determined by gas-chromatographic analysis. Integration times of 100 s

for the polarized component and 200 s for the depolarized component were used to record the depolarization ratios given in Table 10.8. Typical polarized and depolarized counts with inclusion of the vibrational Raman lines at 86 °C and ≈ 15 kPa were 17 282 and 55 cps, with background counts of 43 and 9 cps, respectively. The depolarization ratios with inclusion and exclusion of the vibrational Raman lines were found to be $100\rho_0$ = 0.304 ± 0.015 and $100\rho_0 = 0.279 \pm 0.011$, and these are the first reported depolarization ratios for dioxane. Combining the depolarization ratio of $100\rho_0 = 0.279 \pm 0.011$ with a mean polarizability for 589 nm of $\alpha = 9.56 \pm 0.29$ (± 3% uncertainty assumed) obtained from liquid-phase refractive indices [57] gives $|3\alpha\kappa| = 1.96 \pm 0.07$.

The polarizability components for dioxane were calculated using the CADPAC program. The energy difference between the chair and half-chair conformations is large (≈ 40 kJ mol^{-1} [58-60]) and only the chair conformation has a significant population at room temperature. This conformation was optimized at the SCF level with the 3-21G basis set giving the following geometry: C–C = 0.1523 (0.1523) nm, C–O = 0.1444 (0.1423) nm, C–H = 0.1085/0.1079 (0.1112) nm and ∠COC = 111.8° (112.4°), where the values in parentheses are from an electron diffraction study [61]. There is satisfactory agreement between the experimental and theoretical geometries.

Zero-frequency and optical-frequency polarizabilities were calculated using the 6-31G(+sd+sp) basis set at the SCF and MP2 levels of theory. The optical-frequency polarizabilities at the MP2 level of theory are given in Table 10.9, and corresponding calculations on cyclohexane, obtained from the literature [62], are included. The MP2 corrections were calculated with the finite-field method.

The $\alpha_{\parallel}$ component of cyclohexane is smaller than the $\alpha_{\perp}$ component due to the greater electronic charge density within the ring of the molecule. Similarly, for dioxane the polarizabiilties within the ring, α_{xx} and α_{zz}, are larger than the α_{yy} component. Of the components within the ring α_{xx}, which coincides with the mirror plane, is smaller than α_{zz} because of the presence of the oxygen atoms in the x-direction. Overall, the polarizability components are smaller for dioxane when compared with cyclohexane due to the replacement of the methylene groups by the less polarizable oxygen atoms.

Table 10.8 Depolarization ratios for dioxane.

$100\rho_0$	
0.329 ± 0.007	0.271 ± 0.010[a]
0.306 ± 0.009	0.268 ± 0.010[a]
0.309 ± 0.008	0.269 ± 0.011[a]
0.296 ± 0.018	0.287 ± 0.010[a]
0.288 ± 0.009	0.289 ± 0.010[a]
0.295 ± 0.008	0.291 ± 0.011[a]

[a] Vibrational Raman lines excluded.

Table 10.9 Polarizability components for dioxane and cyclohexane calculated at the MP2 level of theory for 632.8 nm.[a]

dioxane		cyclohexane	
α_{xx}	8.86	$\alpha_{\perp}$	12.253
α_{yy}	8.35	$\alpha_{\parallel}$	10.581
α_{zz}	10.62		
α	9.27		11.69
$\Delta\alpha$	−2.1		−1.67

[a] The cyclohexane values are from reference [62]. For dioxane, the z-axis coincides with the C_2 rotation axis, and the polarizabilities have been transformed into the principal axis system. For cyclohexane, the z-axis coincides with the three-fold axis.

The larger value of the polarizability anisotropy for dioxane reflects the greater inequality of the electronic charge distribution within dioxane relative to cyclohexane. Therefore, the smaller mean polarizability and larger polarizability anisotropy result in a larger depolarization ratio for dioxane. The calculated polarizability anisotropy for dioxane is in good agreement with the experimental value of $|3\alpha\kappa|$, although the mean polarizability is too small by 3%.

Tetrafluorobenzenes

A systematic study of the electric properties of the fluorobenzenes using the gas-phase Kerr effect was commenced by Gentle *et al.* [63,64]. These studies have enabled the separation of the temperature-dependent and temperature-independent contributions to the zero-density Kerr constants, and yielded the polarizabilities for benzene, fluorobenzene, 1,3,5-trifluorobenzene, pentafluorobenzene, and hexafluorobenzene. As a part of this study, the depolarization ratios of 1,2,3,5- and 1,2,4,5-tetrafluorobenzene were measured to assist the analysis of the Kerr effect measurements of Blanch and Ritchie [1].

Samples of 1,2,3,5-tetrafluorobenzene (> 95%) and 1,2,4,5-tetrafluorobenzene (> 99%) were obtained from the Aldrich Chemical Company; 1,2,3,5-tetrafluorobenzene was purified using a procedure from the literature [22] giving a purity of > 98.2% by gas-chromatographic analysis, and 1,2,4,5-tetrafluorobenzene was used without further purification. Both species were subjected to two freeze-pump-thaw cycles immediately before use.

The depolarization ratios for 1,2,3,5- and 1,2,4,5-tetrafluorobenzene are given in Table 10.10, and the vibrational Raman lines were included. Integration times were 300 s for the polarized component and 600 s for the depolarized component. Typical polarized and depolarized counts for 1,2,3,5-tetrafluorobenzene at 86.8 °C and ≈ 23 kPa were 10 395 and 235 cps, with background counts of 18 and 6 cps, respectively. Typical polarized and depolarized counts for 1,2,4,5-tetrafluorobenzene at 86.8 °C and ≈ 26 kPa were 8 237 and 186 cps, with background counts of 23 and 5 cps, respectively. The mean depolarization ratios were found to be $100\rho_0 = 2.18 \pm 0.03$ for 1,2,3,5-tetrafluorobenzene and $100\rho_0 = 2.23 \pm 0.05$ for 1,2,4,5-tetrafluorobenzene. It is noted that the dipole moments for 1,2,3,4-tetrafluorobenzene and 1,2,3,5-tetrafluorobenzene, required in the analysis of the Kerr constants, have recently been been reported [65].

Table 10.10 Depolarization ratios for 1,2,3,5- and 1,2,4,5-tetrafluorobenzene.

$100\rho_0$			
1,2,3,5-tetrafluorobenzene		1,2,4,5-tetrafluorobenzene	
2.183 ± 0.020	2.136 ± 0.019	2.217 ± 0.017	2.233 ± 0.019
2.159 ± 0.016	2.163 ± 0.019	2.240 ± 0.016	2.295 ± 0.023
2.178 ± 0.017	2.203 ± 0.016	2.214 ± 0.019	2.271 ± 0.013
2.205 ± 0.017	2.192 ± 0.016	2.141 ± 0.021	2.268 ± 0.022
		2.196 ± 0.022	

Trimethylboroxine

There has been much interest in the boron, oxygen and nitrogen substituted analogues of benzene [66-78]. In particular, there has been considerable discussion of the degree of π electron delocalization within these ring systems. Studies of the gas-phase electric properties of the nitrogen substituted analogues of benzene are possible, although the vapour pressures are low (Chapter 8). Problems are expected to be encountered with other species such as borazine, which is corrosive. The depolarization ratio for trimethylboroxine was investigated as a first step in the study of the gas-phase electric properties of ring systems containing boron and oxygen.

A sample of trimethylboroxine (> 99%) was obtained from the Aldrich Chemical Company and used without further purification. The sample was subjected to two freeze-pump-thaw cycles immediately before use. The depolarization ratios, with the vibrational Raman lines included, are given in Table 10.11. Typical polarized and depolarized counts with inclusion of the vibrational Raman lines at 87.8 °C and ≈ 35 kPa were 110 270 and 779 cps, with background counts of 30 and 4 cps, respectively. Integration times were 100 s for the polarized component and 200 s for the depolarized component. The mean depolarization ratios, with inclusion and exclusion of the vibrational Raman lines, were found to be $100\rho_0$ = 0.704 ± 0.004 and $100\rho_0$ = 0.695 ± 0.006 and, therefore, the vibrational Raman contribution was negligible.

A mean polarizability was also recorded, with exclusion of the vibrational Raman

lines, giving a value of α = 14.96 ± 0.06. Gas ideality was assumed, since density second virial coefficients are unknown for this compound. Combining the mean polarizability with the depolarization ratio of $100\rho_0$ = 0.695 ± 0.006 gives $\Delta\alpha$ = −4.85 ± 0.03, $\alpha_{\parallel}$ = 11.72 ± 0.07 and $\alpha_{\perp}$ = 16.58 ± 0.06. These results can be compared with the properties of mesitylene (Chapter 5) of $\alpha_{\parallel}$ = 11.64 ± 0.43, $\alpha_{\perp}$ = 21.06 ± 0.37, α = 17.92 ± 0.36 and $\Delta\alpha$ = −9.43 ± 0.23. From the results, it is evident that the presence of the oxygen atoms significantly reduces the out-of-plane polarizability of the ring, whereas the in-plane component is unchanged.

Table 10.11 Depolarization ratios for trimethylboroxine.

$100\rho_0$		
0.708 ± 0.002	0.698 ± 0.003	0.689 ± 0.003[a]
0.700 ± 0.003	0.703 ± 0.003	0.695 ± 0.003[a]
0.706 ± 0.003	0.709 ± 0.003	0.693 ± 0.003[a]
0.703 ± 0.003	0.704 ± 0.003[a]	0.692 ± 0.003[a]

[a] Vibrational Raman lines excluded.

References

1. Blanch, E.W. and Ritchie, G.L.D., unpublished results.
2. Bridge, N.J. and Buckingham, A.D., *Proc. Roy. Soc. A*, **295**, 334 (1966).
3. Alms, G.R., Burnham, A.K. and Flygare, W.H., *J. Chem. Phys.*, **63**, 3321 (1975).
4. Hesling, M.R., *"Measurements of Rayleigh depolarization ratios of gases and vapours."*, Ph.D. Thesis, University of New England, (1990).
5. Lukins, P.B., Laver, D.R., Buckingham, A.D. and Ritchie, G.L.D., *J. Phys. Chem.*, **89**, 1309 (1985).
6. Bogaard, M.P., Buckingham, A.D., Pierens, R.K. and White, A.H., *J. Chem. Soc., Faraday Trans. 1*, **74**, 3008 (1978).
7. Monan, M., Bribes, J.L. and Galfrès, R., *J. Raman Spectrosc.*, **12**, 190 (1982).
8. Dymond, J.H. and Smith, E.B., *'The virial coefficients of pure gases and mixtures"*, (Oxford University Press, Oxford, 1980).
9. Hohm, U., *Chem. Phys.*, **179**, 533 (1994).
10. Hohm, U., *Mol. Phys.*, **81**, 157 (1994).
11. Thomas, G.F., Mulder, F. and Meath, W.J., *Chem. Phys.*, **54**, 45 (1980).
12. Böttcher, O., Meyer, V. and Sutter, D.H., *Z. Naturforsch. A*, **45**, 585 (1994).
13. Aldrich, P.D., Kukolich, S.G., Campbell, E.J. and Read, W.G., *J. Am. Chem. Soc.*, **105**, 5569 (1983).
14. Watson, J.N., *"The measurement of field-gradient induced birefringence in gases"*, Ph.D. Thesis, University of New England, (1994).
15. Buckingham, A.D., Graham, C. and Williams, J.H., *Mol. Phys.*, **49**, 703 (1983).
16. Amos, R.D. and Williams, J.H., *Chem. Phys. Lett.*, **84**, 104 (1981).
17. Spackman, M.A., *J. Phys. Chem.*, **93**, 7594 (1989).
18. Dagg, I.R., Anderson, A., Smith, W., Reid, P.J., Joslin, C.G. and Gray, C.G., *Can. J. Phys.*, **70**, 134 (1992)
19. Ritchie, G.L.D., Spackman, M A. and Stankey, R., unpublished results.
20. Jones, K.M., Keir, R.I., Ritchie, G.L.D. and Spackman, M.A., unpublished results.

21. Bevington, J.C., *Quart. Rev.*, **6**, 141 (1952).

22. Perrin, D.D., Armarego, W.L.F. and Perrin, D.R., *"Purification of laboratory chemicals"*, 2nd Edition (Pergamon, Oxford, 1980).

23. Walker, J.F., *"Formaldehyde"*, (Reinhold Publishing Company, New York, 1964).

24. Sauer, S.P.A. and Oddershede, J., *Int. J. Quant. Chem.*, **50**, 317 (1994).

25. Landolt-Börnstein, *"Numerical data and functional relationships in science and technology"*, Volume II/8 (Springer-Verlag, Berlin, 1962).

26. Zeiss, G.D., Meath, W.J., MacDonald, J.C.F. and Dawson, D.J., *Can. J. Phys.*, **55**, 2080 (1977).

27. Zeiss, G.D. and Meath, W.J., *Mol. Phys.*, **33**, 1155 (1977).

28. Armstrong, R.S., Aroney, M J., Calderbank, K.E. and Pierens, R.K., *Aust. J. Chem.*, **30**, 1411 (1977).

29. Breazeale, W.M., *Phys. Rev.*, **48**, 237 (1935).

30. Le Fèvre, R.J.W. and Ritchie, G.L.D., *J. Chem. Soc.*, 3520 (1965).

31. Liu, S. and Dykstra, C.E., *J. Phys. Chem.*, **91**, 1749 (1987).

32. Maroulis, G., *Chem. Phys. Lett.*, **195**, 85 (1992).

33. Werner, H.J. and Meyer, W., *Mol. Phys.*, **31**, 855 (1976).

34. Diercksen, G.H.F. and Sadlej, A.J., *Mol. Phys.*, **57**, 509 (1986).

35. Spirko, V., Jensen, H.J. and Jørgensen, P., *Chem. Phys.*, **144**, 343 (1990).

36. Reinsch, E.A., *J. Chem. Phys.*, **83**, 5784 (1985).

37. Ritchie, G.L.D. and Stankey, R., unpublished results.

38. Sekino, H. and Bartlett, R.J., *J. Chem. Phys.*, **98**, 3022 (1993).

39. Russell, A.J. and Spackman, M.A., unpublished results.

40. Sadlej, A.J., *Coll. Czech. Chem. Comm.*, **53**, 1995 (1988).

41. Wormer, P.E.S., Olthof, E.H.T., Engeln, R.A.H. and Reuss, J., *Chem. Phys.*, **178**, 189 (1993).

42. Murphy, W.F., *J. Chem. Phys.*, **67**, 5877 (1977).

43. Haverkort, J.E.M., Baas, F. and Beenakker, J.J.M., *Chem. Phys.*, **79**, 105 (1983).

44. Hohm, U. and Kerl, K., *Mol. Phys.*, **58**, 541 (1986).

45. Spelsberg, D. and Meyer, W., *J. Chem. Phys.*, **101**, 1281 (1994).

46. Bishop, D.M. and Cybulski, S M., *J. Chem. Phys.*, **101**, 2180 (1994).

47. Baas, F. and van den Hout, K.D., *Physica*, **95**, 597 (1979).

48. Graham, C., Imrie, D.A. and Raab, R.E., unpublished results.

49. Buckingham, A.D. and Le Fèvre, R.J.W., *J. Chem. Soc.*, **4**, 3432 (1953).

50. Buckingham, A.D., Disch, R.L. and Dunmur, D.A., *J. Am. Chem. Soc.*, **90**, 3104 (1968).

51. Graham, C., Pierrus, J. and Raab, R.E., *Mol. Phys.*, **67**, 939 (1989).

52. Huot, J. and Bose, T.K., *J. Chem. Phys.*, **94**, 3849 (1991).

53. Poll, J.D. and Hunt, J.L., *Can. J. Phys.*, **59**, 1448 (1981).

54. Dagg, I.R., Anderson, A., Yan, S., Smith, W. and Read, L.A.A., *Can. J. Phys.*, **63**, 625 (1985).

55. Budenholzer, F.E., Gislason, E.A., Jorgenson, A.D. and Sachs, J.G., *Chem. Phys. Lett.*, **47**, 429 (1977).

56. Kling, H. and Hüttner, W., *Chem. Phys.*, **90**, 207 (1984).

57. Weast, R.C., *"CRC Handbook of Chemistry and Physics"*, 70th Edition (CRC Press, Boca Raton, 1990).

58. Anet, F.A.L. and Sandstrom, J , *Chem. Comm.*, 1558 (1971).

59. Jensen, F.R. and Neese, R.A., *J. Am. Chem. Soc.*, **93**, 6329 (1971).

60. Jensen, F.R. and Neese, R.A., *J. Am. Chem. Soc.*, **97**, 4345 (1975).

61. Davis, M. and Hassel, O., *Acta Chem. Scand.*, **17**, 1181 (1963).

62. Spackman, M.A., *Chem. Phys Lett.*, **161**, 285 (1989).

63. Gentle, I.R., Hesling, M.R. and Ritchie, G.L.D., *J. Phys. Chem.*, **94**, 1844 (1990).

64. Gentle, I.R. and Ritchie, G.L.D., *J. Phys. Chem.*, **93**, 7740 (1989).

65. Onda, M., Yamada, H., Miyazaki, H., Mori, M. and Yamaguchi, I., *J. Mol. Spectrosc.*, **166**, 247 (1994).

66. Roothaan, C.C.J. and Mulliken, R.S., *J. Chem. Phys.*, **16**, 118 (1948).

67. Davies, D.W., *Trans. Faraday Soc*, **56**, 1713 (1960).

68. Blustin, P.H., *Mol. Phys.*, **36**, 279 (1978).

69. Haddon, R.C., *Pure & Appl. Chem.*, **54**, 1120 (1982).

70. Boyd, R.J., Choi, S.C. and Hale, C.C., *Chem. Phys. Lett.*, **112**, 136 (1984).

71. Cooper, D.L., Wright, S.C., Gerratt, J., Hyams, P.A. and Raimondi, M., *J. Chem. Soc., Perkin Trans. 2*, 719 (1989).

72. Lazzeretti, P., Malagoli, M. and Zanasi, R., *Chem. Phys. Lett.*, **167**, 101 (1990).

73. Lazzeretti, P. and Tossell, J.A. *J. Mol. Struct. (Theochem)*, **236**, 403 (1991).

74. Archibong, E.F. and Thakkar, A.J., *Mol. Phys.*, **81**, 557 (1994).

75. Matsunaga, N., Cundari, T.R. Schmidt, M.W. and Gordon, M.S., *Theor. Chim. Acta.*, **83**, 57 (1992).

76. Boese, R., Maulitz, A.H. and Stellberg, P., *Chem. Ber.*, **127**, 1887 (1994).

77. Dennis, G.R. and Ritchie, G.L.D., *J. Phys. Chem.*, **97**, 8403 (1993).

78. Doering, J.P., Gedanken, A., Hitchcock, A.P., Fischer, P., Moore, J., Olthoff, J.K., Tossell, J., Raghavachari, K. and Robin, M.B., *J. Am. Chem. Soc.*, **108**, 3602 (1986).

Chapter Eleven

Conclusions

Discussion

The depolarization ratio and the mean polarizability, in combination, give values of the polarizability anisotropy ($\sigma \cdot |3\alpha\kappa|$ for low-symmetry species). The accurate determination of the polarizability anisotropy is important, since it is required for the extraction of information from measurements of the Kerr effect, the Cotton-Mouton effect and the field-gradient induced birefringence effect. Furthermore, the polarizability anisotropy gives a direct measure of the distribution of the electronic charge within a molecule, and its response to an external electric field. This final chapter summarizes some of the more important conclusions of the research presented in this thesis.

It has been shown in the present research that measurements of the depolarization ratio, especially at higher temperatures, can usefully elucidate the anisotropic molecular polarizabilities of chemically interesting species. For this reason, the light scattering apparatus was rebuilt with the aim of improving the signal-to-noise ratio while increasing the reliability and stability of the equipment at elevated temperatures. A more powerful laser was installed, and various components of the apparatus were modified to accommodate the laser. Improvements were made to the photon-counting technique by triggering the photon counter directly from a light chopper. Greater stability and more reliable realignment of the light scattering cell was obtained by installing a micrometer-driven positioner.

Considerable effort went into redesigning the gas-handling system, with the aim of reducing pressure and temperature inhomogeneities along the tubing and ensuring stable operation at elevated temperatures. The overall improvement was scattering intensities that were a factor of three larger than with the previous design, a gas-handling system that was easily dismantled and cleaned, higher operating temperatures, and a significant reduction in down-time.

The depolarization ratios for carbon dioxide, nitrogen, acetylene, and benzene were used to check the apparatus, and these were found to be in excellent agreement with the best literature values. From a study of the depolarization ratio of argon, the instrumental depolarization of the apparatus was found to be negligible. In consequence, the other depolarization ratios determined in this research were not corrected for an instrumental depolarization. Where appropriate, the depolarization ratios were recorded with exclusion of the vibrational Raman intensities. Considerable effort was made to ensure that dust-free, high-purity samples were examined.

Part of the research presented in this thesis was aimed at studying species which were of interest to Mr E.W. Blanch and Dr J.N. Watson for their doctoral research on the Kerr effect and the field-gradient induced birefringence effect, respectively. Some of the research involved filling in the missing pieces for series of molecules, for example, the results obtained for fluoroethane complement the research on the other halogenated ethanes previously undertaken by Ritchie *et al* [1]. Another aim was to study interesting species which posed an experimental challenge, for example, formaldehyde and the boron trihalides.

It was decided at the outset to record, where possible, mean polarizabilities for each molecule, and compare the results with known literature values. It was hoped that this would provide information as to the accuracy and precision of mean polarizabilities recorded with the light scattering equipment. The mean polarizabilities obtained in the present research are compared with preferred values in Table 11.1. Preferred values were generally obtained from gas- or liquid-phase refractive indices. The absence of a preferred value implies that the mean polarizability obtained from light scattering is within

1% of the literature values. For dimethylacetylene, the preferred value was taken from Bogaard *et al.* [2], where the dispersion in the mean polarizability for dimethylacetylene was assumed to be the same as the dispersion in the mean polarizability of methylacetylene. For hexafluoroethane, the value reported by Bulanin *et al.* [3] was preferred, after consideration of the ab initio calculations. The mean polarizability for boron trifluoride obtained in the present research seems to be too low, and the value for boron trichloride seems to be too high. This may indicate that the samples used in the determination of the original refractive indices were impure; however, this point has been ignored in the analyses given in Chapter 4. A redetermination of the refractive indices would resolve the discrepancies.

Overall, mean polarizabilities obtained by the light scattering method are slightly high compared to the preferred values. Furthermore, it is expected that the mean polarizabilities of vapours would be less precise due to the restricted pressure range, although a value for pyridine (Chapter 8) determined in the present research was satisfactory. It was thought prudent to use mean polarizabilities obtained from refractive indices rather than the present values, since it is generally believed, and shown to be the case here, that mean polarizabilities derived from refractive indices are of a higher accuracy. In most cases only one mean polarizability was recorded for each molecule, so that the uncertainties given may be optimistic. Conservative uncertainties have been assumed for some of the mean polarizabilities given in Table 11.1, and these have been explicitly stated for each molecule in the preceding chapters.

Table 11.1 also includes a summary of the percentage contributions to the depolarization ratios from the vibrational Raman lines. For species such as the xylenes and the diazines this contribution was ignored, since the depolarization ratios are large. It is well known that, for the smaller and less anisotropic species, the vibrational Raman lines must be excluded or the polarizability anisotropies derived from the depolarization ratios will be too large. From Table 11.1, it is evident that for species such as ammonia, cyclopropane, ethane, hexafluoroethane, and nitrogen the vibrational Raman lines do make a significant contribution to the depolarization ratios. Therefore, for several

species, the electric and magnetic properties were reanalyzed by taking into account the lower polarizability anisotropies now available.

Table 11.1 Comparison of the present mean polarizabilities at 632.8 nm and preferred values, and the vibrational Raman contribution to the depolarization ratio for each molecule.

Molecule	Light scattering α	Preferred value α	Percentage difference (%)	vib. Raman contribution to ρ_0 (%)
CO_2	2.97 ± 0.03	2.93 ± 0.09	+1.4	0.5
OCS	5.95 ± 0.03	5.78 ± 0.17	+2.9	0.5
BF_3	2.59 ± 0.13	2.71 ± 0.08	−4.4	3.2
BCl_3	9.77 ± 0.49	9.16 ± 0.27	+6.6	0.8
C_2H_6	5.00 ± 0.05			20
C_2H_5F	5.02 ± 0.02			16
C_2F_6	5.66 ± 0.03	5.37 ± 0.15	+5.4	32
HC≡CH	3.98 ± 0.04	3.88 ± 0.08	+2.6	4.0
$CH_3C{\equiv}CH$	6.41 ± 0.07	6.35 ± 0.15	+1	5.8
$CH_3C{\equiv}CCH_3$	8.81 ± 0.09	8.19 ± 0.16	+7.6	1.5
CH_3Br	6.42 ± 0.06	6.22 ± 0.06	+3.2	2.7
CH_2Br_2	9.59 ± 0.10			2.6
C_3H_6	6.55 ± 0.02	6.28 ± 0.06	+4.3	20
NH_3	2.49 ± 0.02			40
N_2	1.964 ± 0.002			7.1

Unexpectedly, the depolarization ratio for carbon disulfide was found to have a pressure dependence, even at pressures below ≈ 100 kPa. A study of the density dependence of the depolarization ratio of carbon disulfide was completed and a zero-density depolarization ratio was determined which agreed with the ratio reported by Alms

et al. [4] and not the ratio reported by Bogaard *et al* [2]. A value for the light scattering second virial coefficient was also determined for carbon disulfide. Surprisingly, the depolarization ratio for carbonyl sulfide determined in the present research was found to agree with the ratio reported by Bogaard *et al.* and not the value reported by Alms *et al.* The pressure dependence of depolarization ratios is well known [5-7].

The depolarization ratio for ethane was remeasured with the aim of resolving the discrepancy amongst the literature values. From Table 11.1, the exclusion of the vibrational Raman lines is necessary to obtain a reliable depolarization ratio and polarizability anisotropy. The present depolarization ratio disagrees with a recent value reported by Coonan [8] from a combination of Cotton-Mouton effect and field-gradient birefringence studies, and a number of other literature values. More research is required to resolve the discrepancies amongst the values, although the present research supports larger values for the depolarization ratio and the polarizability anisotropy.

The ab initio calculations reported in this thesis were included to complement the experimental results and are not claimed to be definitive, since vibrational averaging, higher-order electron correlation, and large basis sets were not used. This was a limitation imposed by the size of the molecules studied. For the diazines, the computational results gave some insight into the change in the polarizability as a function of nitrogen substitution into the benzene ring. An experimental determination of the polarizabilities awaits measurement of the Kerr effects of these species. The polarizabilities calculated for the boron trihalides and bromomethanes were found to be in good agreement with the experimental values.

The research reported in this thesis has provided new information about the electric properties of some species, and enabled the reanalysis of the electric and magnetic properties of others. There is still a great deal of scope for light scattering measurements of other chemically interesting species. The electric and magnetic properties of borazine, the boron-nitrogen analogue of benzene, are of interest in relation to the extent of electron delocalization in this molecule. The reactivity and corrosive nature of this compound would make the measurement of the depolarization ratio a challenge. Other interesting

species include, the acetyl halides, acetyl cyanide, acetic acid, and thioacetic acid. In these cases, the aim would be to stuc ly the changes in the electric properties of the species when various functional groups are attached to the acetyl group.

The present apparatus was c perated safely at 90 °C; with slight modifications to some of the components it should be possible to raise the operating temperature to ≈ 150 °C and measure the depolarization ratios of less volatile species such as the dichloro- and dibromobenzenes. Furthermo e, a remeasurement of the depolarization ratios of other dense vapours such as mesitylene and *s*-triazine at higher temperatures would improve the reliability of the electric and magnetic properties of these species.

There are a number of modif cations which could be made to the present apparatus such as reducing the size of the o ven, minimizing the leakage of stray light into the apparatus and automating some of t ne alignment procedures. However, it is evident that higher powered lasers and more sensitive photomultiplier tubes will give the larger scattering signals required to incr ease the precision of the equipment. Finally, the equipment could easily be modified to permit the analysis of the frequency dependence of the depolarization ratio and of the vibrational Raman lines, since this is an area where there is a distinct lack of experiment al data.

References

1. Ritchie, G.L.D., Spackman, M.A. and Stankey, R., unpublished results.
2. Bogaard, M.P., Buckingham, A D., Pierens, R.K. and White, A.H., *J. Chem. Soc., Faraday Trans. 1*, **74**, 3008 (1978).
3. Bulanin, M.O., Burtsev, A.P. and Tretyakov, P.Y., *Opt. Spectrosc. (USSR)*, **69**, 760 (1990).
4. Alms, G.R., Burnham, A.K. and Flygare, W.H., *J. Chem. Phys.*, **63**, 3321 (1975).
5. Dayan, E., Dunmur, D.A. and Manterfield, M.R., *J. Chem. Soc., Faraday Trans. 2*, **76**, 309 (1980).
6. Couling, V.W. and Graham, C., *Mol. Phys.*, **79**, 859 (1993).
7. Couling, V.W. and Graham, C., *Mol. Phys.*, **82**, 235 (1994).
8. Coonan, M.H., *"Temperature dependence of the Cotton-Mouton effect in gases"*, Ph.D. Thesis, University of New England, (1995).

Appendix I

This Appendix contains tables of polarizabilities as a function of frequency for some of the molecules studied in the present research. The tables are as follows: Tables A1–A4, boron trifluoride, boron trichloride, boron tribromide and boron triiodide; Table A5, hexafluoroethane; Tables A6–A11, acetylene, methylacetylene and dimethylacetylene; Tables A12–A23, benzene, pyridine, pyridazine, pyrimidine, pyrazine and *s*-triazine; Tables A24–A28, methane, bromomethane, dibromomethane, tribromomethane and tetrabromomethane.

It is noted that the optical-frequency MP2 values are not exact, but are estimated by applying a correction obtained from the difference between the MP2 and SCF zero-frequency calculations to the optical frequency SCF values.

The polarizabilities were calculated with the following basis sets:

1. The 6-31G(+sd+sp) basis set as specified by Spackman [1].
2. The 6-31G(+pd+sp) basis set. A modified form of the above basis set where the s function on the heavy atom has been replaced by a p function with the same exponent. For planar, highly conjugated molecules this allowed greater polarization out of the plane of the molecule with a minimal increase in computational effort.
3. The HUZ-SV(+sd+sp) basis set as specified by Dougherty and Spackman [2]. This basis set was required for the calculations on the boron trihalides and bromomethanes, because they include heavy atoms which are not specified in the 6-31G(+sd+sp) basis set.
4. It is noted that in the case of the acetylenes it was necessary in some cases to modify the d exponent for the 6-31G(+sd+sp) basis set to obtain convergence of the energy. The modification is noted in each table and is analyzed in Chapter 7.

Ab initio polarizabilities of the boron trihalides using the HUZI(+sd) basis set at the SCF and MP2 levels of theory. Calculations using the 6-31G(+pd) basis set are included for BF_3 and BCl_3, see Chapter 4 for a comment on these results. Geometries used in the calculations are given in Chapter 4.

Table A1 Polarizabilities for BF_3 at the SCF and MP2 levels of theory.[a]

	SCF				MP2[b]			
λ(nm)	$\alpha_\perp$	$\alpha_{\parallel}$	α	$\Delta\alpha$	$\alpha_\perp$	$\alpha_{\parallel}$	α	$\Delta\alpha$
∞	2.271	1.761	2.101	−0.501	2.714	2.040	2.489	−0.674
	2.327	*1.839*	*2.165*	*−0.488*	*2.798*	*2.155*	*2.584*	*−0.643*
647	2.287	1.772	2.116	−0.515	2.730	2.051	2.504	−0.680
	2.345	*1.851*	*2.180*	*−0.493*	*2.816*	*2.168*	*2.599*	*−0.648*
632	2.288	1.773	2.116	−0.515	2.731	2.051	2.505	−0.680
	2.346	*1.852*	*2.181*	*−0.494*	*2.816*	*2.168*	*2.600*	*−0.648*
568	2.292	1.776	2.120	−0.517	2.508	2.054	2.508	−0.681
	2.350	*1.855*	*2.185*	*−0.495*	*2.821*	*2.171*	*2.604*	*−0.651*
514	2.297	1.779	2.124	−0.518	2.740	2.058	2.513	−0.683
	2.355	*1.858*	*2.189*	*−0.497*	*2.826*	*2.175*	*2.609*	*−0.651*
488	2.300	1.781	2.127	−0.519	2.743	2.060	2.515	−0.684
	2.358	*1.861*	*2.192*	*−0.498*	*2.829*	*2.177*	*2.612*	*−0.652*
457	2.304	1.784	2.131	−0.521	2.747	2.062	2.519	−0.685
	2.362	*1.864*	*2.196*	*−0.499*	*2.833*	*2.180*	*2.615*	*−0.654*

[a] Values in italics were calculated with the 6-31G(+pd) basis set as a comparison.

Table A2 Polarizabilities for BCl_3 at the SCF and MP2 levels of theory.[a]

	SCF				MP2			
λ(nm)	$\alpha_\perp$	$\alpha_\parallel$	α	$\Delta\alpha$	$\alpha_\perp$	$\alpha_\parallel$	α	$\Delta\alpha$
∞	8.885	6.031	7.934	−2.853	10.066	6.521	8.884	−3.545
	8.952	*6.124*	*8.009*	*−2.828*	*10.169*	*6.656*	*8.998*	*−3.513*
647	9.051	6.113	8.072	−2.939	10.232	6.602	9.022	−3.630
	9.122	*6.207*	*8.150*	*−2.914*	*10.338*	*6.689*	*9.139*	*−3.600*
632	9.059	6.117	8.078	−2.943	10.240	6.606	9.029	−3.634
	9.129	*6.211*	*8.157*	*−2.918*	*10.346*	*6.743*	*9.145*	*−3.604*
568	9.102	6.138	8.114	−2.965	10.284	6.627	9.065	−3.656
	9.174	*6.232*	*8.193*	*−2.941*	*10.391*	*6.764*	*9.182*	*−3.677*
514	9.152	6.161	8.155	−2.991	10.333	6.651	9.106	−3.682
	9.224	*6.257*	*8.235*	*−2.967*	*10.441*	*6.788*	*9.224*	*−3.653*
488	9.184	6.176	8.181	−3.007	10.365	6.666	9.132	−3.698
	9.256	*6.272*	*8.261*	*−2.984*	*10.473*	*6.804*	*9.250*	*−3.669*
457	9.226	6.197	8.216	−3.029	10.407	6.687	9.167	−3.721
	9.300	*6.293*	*8.297*	*−3.007*	*10.517*	*6.823*	*9.286*	*−3.692*

[a] Values in italics were calculated with the 6-31G(−pd) basis set as a comparison.

Table A3 Polarizabilities for BBr_3 at the SCF and MP2 levels of theory.

	SCF				MP2			
λ(nm)	$\alpha_\perp$	$\alpha_\parallel$	α	$\Delta\alpha$	$\alpha_\perp$	$\alpha_\parallel$	α	$\Delta\alpha$
∞	12.977	8.572	11.509	−4.405	14.705	9.267	12.892	−5.438
647	13.312	8.726	11.783	−4.586	15.040	9.421	13.167	−5.620
632	13.328	8.733	11.796	−4.595	15.056	9.428	13.180	−5.628
568	13.416	8.773	11.869	−4.643	15.144	9.468	13.252	−5.677
514	13.518	8.819	11.952	−4.700	15.246	9.513	13.335	−5.733
488	13.583	8.847	12.004	−4.735	15.311	9.542	13.388	−5.768
457	13.671	8.887	12.076	−4.784	15.399	9.581	13.460	−5.818

Table A4 Polarizabilities for BI_3 at the SCF and MP2 levels of theory.

	SCF				MP2			
λ(nm)	$\alpha_\perp$	$\alpha_\parallel$	α	$\Delta\alpha$	$\alpha_\perp$	$\alpha_\parallel$	α	$\Delta\alpha$
∞	20.527	13.137	18.064	−7.390	23.178	14.043	20.133	−9.316
647	21.313	13.458	18.695	−7.855	23.964	14.364	20.764	−9.600
632	21.351	13.473	18.725	−7.878	24.001	14.379	20.794	−9.623
568	21.563	13.557	18.895	−8.006	24.214	14.463	20.963	−9.751
514	21.811	13.654	19.092	−8.157	24.462	14.560	21.161	−9.902
488	21.969	13.715	19.218	−8.254	24.620	14.621	21.287	−9.999
457	22.189	13.799	19.392	−8.390	24.840	14.704	21.461	−10.135

Ab initio polarizabilities for hexafluoroethane using the 6-31G(+sd+sp) basis set at the SCF and MP2 levels of theory. Zero-frequency SCF and MP2 polarizability components for ethane are given in reference [1] and are quoted in Chapter 6. The geometry used in the calculations is given in Chapter 6.

Table A5 Polarizabilities for hexafluoroethane using the 6-31G(+sd+sp) basis set.

	SCF				MP2			
λ(nm)	$\alpha_\perp$	$\alpha_\parallel$	α	$\Delta\alpha$	$\alpha_\perp$	$\alpha_\parallel$	α	$\Delta\alpha$
∞	4.570	4.372	4.504	−0.193	5.115	4.928	5.053	−0.187
647	4.602	4.403	4.536	−0.199	5.148	4.960	5.085	−0.188
632	4.604	4.405	4.538	−0.199	5.149	4.961	5.086	−0.188
568	4.612	4.413	4.546	−0.199	5.157	4.969	5.094	−0.188
514	4.621	4.422	4.555	−0.199	5.167	4.978	5.104	−0.188
488	4.627	4.428	4.561	−0.199	5.172	4.984	5.110	−0.188
457	4.635	4.436	4.569	−0.120	5.180	4.992	5.117	−0.188

Ab initio polarizabilities for acetylene, methylacetylene and dimethylacetylene using the 6-31G(+sd+sp) and 6-31G(+pd+sp) basis sets at the SCF and MP2 levels of theory. The d exponent on the heavy atom has been changed in some cases to obtain convergence of the energy, these are labelled 6-31G(+sd+sp)$_e$ and 6-31G(+pd+sp)$_e$, respectively. The effect of this change is discussed in Chapter 7. Static SCF and MP2 polarizability components for acetylene are given in reference [1]. Geometries used in the calculations are given in Table 7.5.

Table A6 Polarizabilities for acetylene using the 6-31G(+pd+sp) basis set.

	SCF				MP2			
λ(nm)	$\alpha_\perp$	$\alpha_\parallel$	α	$\Delta\alpha$	$\alpha_\perp$	$\alpha_\parallel$	α	$\Delta\alpha$
∞	2.968	5.302	3.746	2.334	2.947	5.072	3.655	2.125
647	3.034	5.444	3.837	2.410	3.013	5.214	3.747	2.201
632	3.037	5.451	3.842	2.414	3.016	5.221	3.751	2.205
568	3.055	5.488	3.866	2.433	3.034	5.258	3.775	2.224
514	3.075	5.531	3.894	2.456	3.054	5.301	3.803	2.247
488	3.088	5.558	3.911	2.471	3.067	5.329	3.821	2.262
457	3.105	5.596	3.935	2.490	3.085	5.366	3.845	2.281

Table A7 Polarizabilities for methylacetylene using the 6-31G(+sd+sp) basis set.

	SCF				MP2			
λ(nm)	$\alpha_\perp$	$\alpha_\parallel$	α	$\Delta\alpha$	$\alpha_\perp$	$\alpha_\parallel$	α	$\Delta\alpha$
∞	4.408	8.189	5.668	3.782	4.463	8.065	5.665	3.602
647	4.486	8.402	5.792	3.915	4.542	8.278	5.787	3.736
632	4.490	8.412	5.797	3.922	4.546	8.288	5.793	3.743
568	4.511	8.468	5.830	3.957	4.566	8.344	5.826	3.778
514	4.535	8.533	5.867	3.998	4.590	8.409	5.863	3.819
488	4.550	8.573	5.891	4.023	4.605	8.449	5.887	3.844
457	4.570	8.629	5.923	4.058	4.626	8.505	5.919	3.879

Table A8 Polarizabilities for methylacetylene using the 6-31G(+pd+sp) basis set.

	SCF				MP2			
λ(nm)	$\alpha_\perp$	$\alpha_\parallel$	α	$\Delta\alpha$	$\alpha_\perp$	$\alpha_\parallel$	α	$\Delta\alpha$
∞	4.563	8.189	5.772	3.626	4.632	8.073	5.779	3.441
647	4.649	8.409	5.903	3.760	4.719	8.294	5.911	3.575
632	4.653	8.420	5.909	3.766	4.723	8.304	5.917	3.581
568	4.676	8.478	5.943	3.801	4.746	8.362	5.951	3.616
514	4.703	8.544	5.983	3.842	4.772	8.429	5.991	3.657
488	4.719	8.587	6.008	3.868	4.789	8.471	6.016	3.682
457	4.742	8.644	6.043	3.903	4.812	8.529	6.051	3.717

Table A9 Polarizabilities for methylacetylene using the 6-31G(+pd+sp)$_e$ basis set. d exponent changed on heavy atom (from 0.175 to 0.25).

	SCF				MP2			
λ(nm)	$\alpha_\perp$	$\alpha_\parallel$	α	$\Delta\alpha$	$\alpha_\perp$	$\alpha_\parallel$	α	$\Delta\alpha$
∞	4.408	8.220	5.678	3.812	4.440	8.119	5.666	3.678
647	4.492	8.444	5.809	3.951	4.524	8.342	5.797	3.817
632	4.496	8.454	5.816	3.958	4.529	8.352	5.803	3.824
568	4.519	8.513	5.850	3.995	4.551	8.411	5.838	3.860
514	4.544	8.581	5.890	4.037	4.577	8.479	5.877	3.903
488	4.560	8.624	5.915	4.063	4.593	8.522	5.902	3.929
457	4.583	8.683	5.949	4.100	4.615	8.581	5.937	3.966

Table A10 Polarizabilities for dimethylacetylene using the 6-31G(+sd+sp)$_e$ basis set. d exponent changed on heavy atom (from 0.175 to 0.25).

	SCF				MP2			
λ(nm)	$\alpha_\perp$	$\alpha_\parallel$	α	$\Delta\alpha$	$\alpha_\perp$	$\alpha_\parallel$	α	$\Delta\alpha$
∞	5.851	11.409	7.703	5.558	5.956	11.405	7.773	5.449
647	5.947	11.711	7.868	5.764	6.053	11.707	7.937	5.651
632	5.952	11.725	7.876	5.773	6.057	11.721	7.945	5.664
568	5.977	11.804	7.919	5.827	6.077	11.800	7.985	5.723
514	6.006	11.895	7.969	5.889	6.112	11.899	8.041	5.787
488	6.024	11.953	8.000	5.928	6.130	11.949	8.070	5.819
457	6.049	12.031	8.043	5.982	6.155	12.028	8.113	5.873

Table A11 Polarizabilities for dimethylacetylene using the 6-31G(+pd+sp)$_e$ basis set. d exponent changed on heavy atom (from 0.175 to 0.25).

	SCF				MP2			
λ(nm)	$\alpha_\perp$	$\alpha_\parallel$	α	$\Delta\alpha$	$\alpha_\perp$	$\alpha_\parallel$	α	$\Delta\alpha$
∞	6.034	11.437	7.835	5.403	6.145	11.464	7.918	5.319
647	6.138	11.748	8.008	5.610	6.249	11.775	8.091	5.526
632	6.143	11.763	8.016	5.620	6.254	11.790	8.099	5.536
568	6.170	11.844	8.061	5.675	6.281	11.872	8.145	5.590
514	6.201	11.939	8.114	5.738	6.313	11.966	8.197	5.653
488	6.221	11.998	8.147	5.777	6.332	12.025	8.230	5.693
457	6.248	12.079	8.192	5.832	6.359	12.107	8.275	5.747

Ab initio polarizabilities for benzene, pyridine, pyridazine, pyrimidine, pyrazine, and *s*-triazine using the 6-31G(+sd+sp) and 6-31G(+pd+sp) basis sets at the SCF and MP2 level of theory. Geometries used in the calculations are given in Table 8.3.

Table A12 Polarizabilities for pyridine using the 6-31G(+sd+sp) basis set.[a]

	SCF					MP2				
λ(nm)	α_{xx}	α_{yy}	α_{zz}	α	$\Delta\alpha$	α_{xx}	α_{yy}	α_{zz}	α	$\Delta\alpha$
∞	12.178	11.404	6.339	9.974	−5.493	12.595	11.879	6.454	10.309	−5.816
647	12.577	11.758	6.457	10.264	−5.755	12.994	12.233	6.572	10.600	−6.078
632	12.597	11.775	6.462	10.264	−5.768	13.013	12.250	6.577	10.614	−6.091
568	12.705	11.870	6.493	10.355	−5.840	13.122	12.345	6.608	10.692	−6.162
514	12.832	11.982	6.529	10.443	−5.924	13.249	12.457	6.644	10.783	−6.246
488	12.913	12.052	6.552	10.505	−5.977	13.330	12.527	6.667	10.841	−6.300
457	13.026	12.150	6.583	10.587	−6.053	13.443	12.625	6.698	10.922	−6.375

[a] The sign of $\Delta\alpha$ has been assumed.

Table A13 Polarizabilities for pyridine using the 6-31G(+pd+sp) basis set.[a]

	SCF					MP2				
λ(nm)	α_{xx}	α_{yy}	α_{zz}	α	$\Delta\alpha$	α_{xx}	α_{yy}	α_{zz}	α	$\Delta\alpha$
∞	12.240	11.475	6.586	10.100	−5.313	12.665	11.991	6.788	10.481	−5.571
647	12.652	11.840	6.716	10.403	−5.575	13.077	12.356	6.918	10.783	−5.832
632	12.672	11.858	6.722	10.417	−5.587	13.097	12.373	6.924	10.798	−5.845
568	12.784	11.956	6.757	10.499	−5.659	13.209	12.472	6.959	10.880	−5.917
514	12.919	12.071	6.797	10.594	−5.744	13.341	12.586	6.998	10.975	−6.001
488	13.000	12.143	6.822	10.655	−5.798	13.425	12.659	7.024	11.036	−6.055
457	13.118	12.244	6.856	10.739	−5.873	13.543	12.760	7.058	11.120	−6.131

[a] The sign of $\Delta\alpha$ has been assumed.

Table A14 Polarizabilities for pyridazine using the 6-31G(+sd+sp) basis set.[a]

	SCF					MP2				
λ(nm)	α_{xx}	α_{yy}	α_{zz}	α	$\Delta\alpha$	α_{xx}	α_{yy}	α_{zz}	α	$\Delta\alpha$
∞	10.454	11.159	5.815	9.14[illegible]	−5.029	10.933	11.549	5.965	9.482	−5.303
647	10.774	11.481	5.931	9.39[illegible]	−5.232	11.253	11.871	6.081	9.735	−5.507
632	10.789	11.497	5.937	9.40[illegible]	−5.242	11.269	11.886	6.087	9.747	−5.516
568	10.876	11.583	5.969	9.47[illegible]	−5.296	11.355	11.972	6.119	9.816	−5.570
514	10.977	11.683	6.008	9.55[illegible]	−5.358	11.457	12.073	6.158	9.896	−5.633
488	11.042	11.747	6.032	9.60[illegible]	−5.397	11.521	12.137	6.183	9.947	−5.672
457	11.131	11.835	6.067	9.67[illegible]	−5.450	11.611	12.225	6.218	10.018	−5.725

[a] The sign of $\Delta\alpha$ has been assumed.

Table A15 Polarizabilities for pyridazine using the 6-31G(+pd+sp) basis set.[a]

	SCF					MP2				
λ(nm)	α_{xx}	α_{yy}	α_{zz}	α	$\Delta\alpha$	α_{xx}	α_{yy}	α_{zz}	α	$\Delta\alpha$
∞	10.546	11.211	6.028	9.26[illegible]	−4.88[illegible]	11.050	11.617	6.253	9.640	−5.104
647	10.877	11.541	6.153	9.52[illegible]	−5.08[illegible]	11.380	11.946	6.378	9.901	−5.308
632	10.893	11.557	6.159	9.53[illegible]	−5.09[illegible]	11.396	11.962	6.384	9.914	−5.317
568	10.982	11.645	6.194	9.60[illegible]	−5.15[illegible]	11.486	12.050	6.419	9.985	−5.371
514	11.087	11.748	6.235	9.69[illegible]	−5.214	11.590	12.153	6.460	10.068	−5.434
488	11.154	11.814	6.262	9.74[illegible]	−5.25[illegible]	11.657	12.219	6.487	10.121	−5.473
457	11.247	11.904	6.299	9.81[illegible]	−5.307	11.750	12.309	6.524	10.194	−5.527

[a] The sign of $\Delta\alpha$ has been assumed.

Table A16 Polarizabilities for pyrimidine using the 6-31G(+sd+sp) basis set.[a]

	SCF					MP2				
λ(nm)	α_{xx}	α_{yy}	α_{zz}	α	$\Delta\alpha$	α_{xx}	α_{yy}	α_{zz}	α	$\Delta\alpha$
∞	10.397	10.824	5.714	8.978	−4.911	10.942	11.469	5.906	9.439	−5.319
647	10.708	11.123	5.811	9.214	−5.117	11.253	11.768	6.004	9.675	−5.525
632	10.723	11.137	5.816	9.226	−5.127	11.268	11.782	6.008	9.686	−5.535
568	10.807	11.217	5.842	9.289	−5.183	11.352	11.862	6.034	9.749	−5.590
514	10.906	11.310	5.872	9.363	−5.248	11.450	11.955	6.064	9.823	−5.655
488	10.968	11.369	5.891	9.409	−5.289	11.513	12.013	6.083	9.870	−5.696
457	11.055	11.450	5.917	9.474	−5.346	11.600	12.095	6.110	9.935	−5.754

[a] The sign of $\Delta\alpha$ has been assumed.

Table A17 Polarizabilities for pyrimidine using the 6-31G(+pd+sp) basis set.[a]

	SCF					MP2				
λ(nm)	α_{xx}	α_{yy}	α_{zz}	α	$\Delta\alpha$	α_{xx}	α_{yy}	α_{zz}	α	$\Delta\alpha$
∞	10.487	10.875	5.914	9.092	−4.779	11.066	11.540	6.187	9.598	−5.133
647	10.807	11.181	6.020	9.335	−4.985	11.387	11.846	6.293	9.842	−5.338
632	10.823	11.196	6.025	9.343	−4.995	11.402	11.861	6.298	9.854	−5.348
568	10.910	11.277	6.053	9.413	−5.050	11.489	11.943	6.326	9.919	−5.404
514	11.011	11.373	6.086	9.493	−5.116	11.591	12.038	6.359	9.996	−5.469
488	11.076	11.433	6.107	9.539	−5.157	11.656	12.098	6.380	10.045	−5.510
457	11.166	11.516	6.135	9.606	−5.215	11.745	12.182	6.409	10.112	−5.568

[a] The sign of $\Delta\alpha$ has been assumed.

Table A18 Polarizabilities for pyrazine using the 6-31G(+sd+sp) basis set.[a]

	SCF					MP2				
λ(nm)	α_{xx}	α_{yy}	α_{zz}	α	$\Delta\alpha$	α_{xx}	α_{yy}	α_{zz}	α	$\Delta\alpha$
∞	11.775	10.044	5.767	9.162	−5.453	12.039	10.588	5.883	9.503	−5.574
647	12.210	10.338	5.874	9.474	−5.639	12.474	10.882	5.990	9.782	−5.853
632	12.232	10.352	5.879	9.483	−5.653	12.496	10.897	5.995	9.796	−5.867
568	12.353	10.431	5.908	9.564	−5.731	12.617	10.976	6.024	9.872	−5.944
514	12.497	10.523	5.942	9.654	−5.824	12.761	11.068	6.059	9.962	−6.037
488	12.590	10.582	5.964	9.712	−5.884	12.854	11.126	6.081	10.020	−6.096
457	12.721	10.663	5.995	9.793	−5.969	12.984	11.207	6.112	10.101	−6.179

[a] The sign of $\Delta\alpha$ has been assumed.

Table A19 Polarizabilities for pyrazine using the 6-31G(+pd+sp) basis set.[a]

	SCF					MP2				
λ(nm)	α_{xx}	α_{yy}	α_{zz}	α	$\Delta\alpha$	α_{xx}	α_{yy}	α_{zz}	α	$\Delta\alpha$
∞	11.834	10.117	5.964	9.305	−5.227	12.109	10.695	6.498	9.768	−5.054
647	12.283	10.419	6.078	9.593	−5.514	12.558	10.997	6.613	10.056	−5.339
632	12.305	10.433	6.084	9.603	−5.528	12.580	11.011	6.618	10.070	−5.353
568	12.431	10.514	6.155	9.687	−5.609	12.706	11.093	6.649	10.149	−5.433
514	12.580	10.609	6.152	9.780	−5.705	12.855	11.187	6.686	10.243	−5.528
488	12.677	10.669	6.175	9.840	−5.766	12.952	11.187	6.709	10.283	−5.574
457	12.813	10.754	6.208	9.925	−5.853	13.088	11.332	6.743	10.387	−5.674

[a] The sign of $\Delta\alpha$ has been assumed.

Table A20 Polarizabilities for benzene using the 6-31G(+pd+sp) basis set.

	SCF				MP2			
λ(nm)	$\alpha_\perp$	$\alpha_\parallel$	α	$\Delta\alpha$	$\alpha_\perp$	$\alpha_\parallel$	α	$\Delta\alpha$
∞	13.082	7.316	11.160	−5.767	13.448	8.058	11.652	−5.390
647	13.537	7.475	11.516	−6.062	13.903	8.217	12.008	−5.685
632	13.559	7.483	11.533	−6.076	13.925	8.225	12.025	−5.700
568	13.682	7.525	11.630	−6.157	14.048	8.267	12.121	−5.781
514	13.826	7.574	11.742	−6.252	14.192	8.316	12.234	−5.876
488	13.918	7.605	11.814	−6.313	14.284	8.347	12.305	−5.937
457	14.045	7.648	11.913	−6.398	14.411	8.390	12.404	−6.021

Table A21 Polarizabilities for benzene using the 6-31G(+sd+sp) basis set.

	SCF				MP2			
λ(nm)	$\alpha_\perp$	$\alpha_\parallel$	α	$\Delta\alpha$	$\alpha_\perp$	$\alpha_\parallel$	α	$\Delta\alpha$
∞	13.011	7.028	11.017	−5.984	13.360	7.103	11.274	−6.256
647	13.451	7.172	11.358	−6.280	13.799	7.248	11.615	−6.552
632	13.472	7.178	11.374	−6.294	13.821	7.254	11.632	−6.566
568	13.591	7.217	11.466	−6.375	13.940	7.293	11.724	−6.647
514	13.730	7.261	11.574	−6.469	14.078	7.337	11.831	−6.742
488	13.819	7.289	11.642	−6.530	14.167	7.365	11.899	−6.802
457	13.941	7.327	11.737	−6.614	14.289	7.403	11.994	−6.886

Table A22 Polarizabilities for *s*-triazine using the 6-31G(+pd+sp) basis set.

	SCF				MP2			
λ(nm)	$\alpha_{\perp}$	$\alpha_{\parallel}$	α	$\Delta\alpha$	$\alpha_{\perp}$	$\alpha_{\parallel}$	α	$\Delta\alpha$
∞	8.499	4.748	7.249	−3.751	9.225	5.093	7.847	−4.132
647	8.707	4.826	7.414	−3.881	9.433	5.171	7.987	−4.262
632	8.717	4.830	7.422	−3.887	9.443	5.175	8.020	−4.268
568	8.772	4.851	7.465	−3.921	9.498	5.196	8.064	−4.302
514	8.836	4.875	7.516	−3.961	9.562	5.220	8.115	−4.342
488	8.877	4.891	7.548	−3.986	9.603	5.235	8.147	−4.367
457	8.933	4.912	7.592	−4.020	9.658	5.257	8.191	−4.402

Table A23 Polarizabilities for *s*-triazine using the 6-31G(+sd+sp) basis set.

	SCF				MP2			
λ(nm)	$\alpha_{\perp}$	$\alpha_{\parallel}$	α	$\Delta\alpha$	$\alpha_{\perp}$	$\alpha_{\parallel}$	α	$\Delta\alpha$
∞	8.427	4.602	7.152	−3.825	9.119	4.882	7.707	−4.236
647	8.629	4.674	7.311	−3.955	9.322	4.955	7.866	−4.367
632	8.639	4.678	7.319	−3.962	9.331	4.958	7.874	−4.373
568	8.693	4.697	7.361	−3.996	9.385	4.977	7.916	−4.408
514	8.755	4.719	7.410	−4.036	9.447	5.000	7.965	−4.447
488	8.795	4.734	7.442	−4.061	9.487	5.014	7.996	−4.473
457	8.849	4.754	7.484	−4.095	9.541	5.034	8.039	−4.507

Ab initio polarizabilities for methane, bromomethane, dibromomethane, tribromomethane and tetrabromomethane using the HUZ-SV(+sd) basis set at the SCF and MP2 levels of theory. The HUZ-SV** geometries are given in Table 9.4.

Table A24 Polarizabilities for methane using the HUZ-SV(+sd+sp) basis set.

	SCF	MP2
λ(nm)	α	
∞	2.603	2.714
647	2.645	2.755
632	2.647	2.758
568	2.657	2.769
514	2.669	2.781
488	2.677	2.789
457	2.688	2.799

Table A25 Polarizabilities for bromomethane using the HUZ-SV(+sd+sp) basis set.

	SCF				MP2			
λ(nm)	$\alpha_\perp$	$\alpha_\parallel$	α	$\Delta\alpha$	$\alpha_\perp$	$\alpha_\parallel$	α	$\Delta\alpha$
∞	4.901	7.320	5.707	2.419	5.264	7.501	6.010	2.237
647	4.995	7.498	5.830	2.503	5.359	7.679	6.132	2.320
632	4.500	7.506	5.835	2.507	5.363	7.687	6.138	2.324
568	5.024	7.553	5.867	2.529	5.388	7.734	6.170	2.346
514	5.053	7.607	5.904	2.554	5.416	7.787	6.207	2.371
488	5.071	7.640	5.927	2.570	5.434	7.821	6.230	2.387
457	5.095	7.686	5.959	2.591	5.459	7.867	6.262	2.408

Table A26 Polarizabilities for dibromomethane using the HUZ-SV(+sd+sp) basis set.

	SCF					MP2				
λ(nm)	α_{xx}	α_{yy}	α_{zz}	α	$\Delta\alpha$	α_{xx}	α_{yy}	α_{zz}	α	$\Delta\alpha$
∞	12.014	6.949	7.849	8.93[illegible]	4.68[illegible]	12.494	7.548	8.351	9.464	4.597
647	12.364	7.082	7.986	9.14[illegible]	4.893	12.844	7.681	8.500	9.675	4.806
632	12.381	7.088	7.993	9.15[illegible]	4.903	12.860	7.687	8.507	9.685	4.816
568	12.473	7.123	8.032	9.20[illegible]	4.958	12.953	7.722	8.545	9.740	4.871
514	12.580	7.163	8.076	9.27[illegible]	5.023	13.059	7.762	8.590	9.804	4.936
488	12.647	7.188	8.104	9.31[illegible]	5.063	13.127	7.787	8.618	9.844	4.976
457	12.740	7.223	8.142	9.36[illegible]	5.119	13.219	7.822	8.656	9.899	5.033

Table A27 Polarizabilities for tribromon ethane using the HUZ-SV(+sd+sp) basis set.

	SCF				MP2[a]			
λ(nm)	$\alpha_{\perp}$	$\alpha_{\parallel}$	α	$\Delta\alpha$	$\alpha_{\perp}$	$\alpha_{\parallel}$	α	$\Delta\alpha$
∞	13.685	9.064	12.125	−4.681	14.427	9.773	12.875	−4.654
647	14.054	9.165	12.424	−4.890	14.796	9.933	13.175	−4.863
632	14.072	9.172	12.438	−4.900	14.814	9.941	13.189	−4.873
568	14.169	9.214	12.517	−4.955	14.911	9.982	13.268	−4.929
514	14.282	9.262	12.609	−5.020	15.023	10.030	13.359	−4.993
488	14.353	9.292	12.666	−5.061	15.095	10.060	13.417	−5.035
457	14.451	9.333	12.745	−5.118	15.193	10.101	13.496	−5.092

[a] Derived from a static finite-field calculation using the GAMESS program.

Table A28 Polarizabilities for tetrabromomethane using the HUZ-SV(+sd) basis set.

	SCF	MP2[a]
λ(nm)	α	
∞	15.305	16.2[illegible]7
647	15.700	16.6[illegible]2
632	15.718	16.6[illegible]1
568	15.823	16.7[illegible]6
514	15.944	16.9[illegible]7
488	16.020	16.9[illegible]3
457	16.126	17.0[illegible]9

[a] Derived from a static finite-field calculation using the GAMESS program.

Appendix II

This Appendix contains references for the vibrational Raman spectra of the compounds presented in this thesis. The list is by no means exhaustive or definitive since the spectra were merely checked to ensure the lowest frequency vibration was outside the bandpass of the laser line filter (at 50% maximum transmission, the bandpass was approximately 625 to 640 nm) A vibrational transition below approximately 190 cm^{-1} will begin to contribute to the Rayleigh depolarization ratio (this is dependent on the intensity and depolarization state of the lowest transitions). The data are meaningless for molecules with large ($100\rho_0 > 1.5$) depolarization ratios since the contribution from the vibrational Raman lines becomes negligible, e.g. the diazines.

The molecules and references are as follows: 1,4-dioxane, pyridine, mesitylene, benzene, toluene, *o*-xylene, *m*-xylene, *p*-xylene [3]; cyclopropane [4,5]; carbon disulfide [5,6]; pyrazine, pyrimidine, pyridazine [7]; *s*-triazine [8]; ethane [5]; fluoroethane [9,10]; hexafluoroethane [10,11]; acetylene [5,12]; methylacetylene [5,13,14]; dimethylacetylene [5,15]; bromomethane [3,16,17]; boron trifluoride, boron trichloride [18]; acetaldehyde [19]. Raman spectra were unavailable for trimethylboroxine, 1,2,3,5-tetrafluorobenzene and 1,2,4,5-tetrafluorobenzene.

For hexafluoro-2-butyne [20], the filter includes approximately 25% of two low frequency bands, one is the 186 cm^{-1} band which corresponds to the C-C-C bend and is intense (most intense of the Raman spectrum) and depolarized (the other band can probably be ignored). This may contribute to the filtered depolarization ratio, but without precise knowledge of the depolarization ratio (only qualitative depolarizations are given in reference [20]) the effect of this line cannot be determined.

For dibromomethane [3,16,21], the filter includes approximately 25% of a low intensity transition at 174 cm^{-1} with a depolarization ratio of 0.35, but since the intensity is low its contribution to the depolarization ratio should be small.

For tribromomethane, the filter includes approximately 25% of a low intensity transition at 154 cm^{-1} with a depolarization ratio of 6/7. As for dibromomethane, since the intensity is low its contribution to the depolarization ratio should be small.

For boron tribromide, the filter includes approximately 30% of an intense low frequency vibration at 151 cm^{-1} [22.23]. The contribution to the Rayleigh depolarization ratio cannot be quantified without knowledge of the depolarization state of the line.

References

1. Spackman, M.A., *J. Phys. Chem.*, **93**, 7594 (1989).
2. Dougherty, J. and Spackman, M.A., *Mol. Phys.*, **82**, 193 (1994).
3. Dollish, F.R., Fateley, W.G. and Bentley, F.F., *"Characteristic Raman frequencies of organic molecules"*, (John Wiley & Sons, New York, 1974).
4. Mathai, P.M., Shepherd, G.G. and Welsh, H.L., *Can. J. Phys.*, **34**, 1448 (1956).
5. Herzberg, G., *"Molecular spectra and molecular structure"*, (Van Nostrand Company, Toronto, 1945).
6. Stoicheff, B.P., *Can. J. Phys.*, **36**, 218 (1958).
7. Lord, R.C., Marston, A.L. and Miller, F.A., *Spectrochim. Acta*, **9**, 113 (1957).
8. Lancaster, J.E., Stamm, R.F. and Colthup, N.B., *Spectrochim. Acta*, **17**, 155 (1961).
9. Smith, D.C., Saunders, R.A., Nielsen, J.R. and Ferguson, E.E., *J. Chem. Phys.*, **20**, 847 (1952).
10. Brown, J.K. and Morgan, K.J., The vibrational spectra of organic fluorine compounds. In *"Advances in fluorine chemistry"*, Stacey, M., Tatlow, J.C. and Sharpe, A.G. (Eds.), (Butterworths, London, 1965),
11. Rank, D.H. and Pace, E.L., *J. Chem. Phys.*, **15**, 39 (1947).
12. Glockler, G. and Renfrew, M.M., *J. Chem. Phys.*, **6**, 340 (1938).
13. Priebe, H., Nielsen, C.J. and Klaeboe, P., *Spectrochim. Acta A*, **36**, 1017 (1980).
14. Crawford, B.L., *J. Chem. Phys.*, **8**, 526 (1940).
15. Crawford, B.L., *J. Chem. Phys.*, **7**, 555 (1939).
16. Long, D.A. and Milner, D.C., *Trans. Faraday Soc.*, **54**, 1 (1958).
17. Welsh, H.L., Crawford, M.F., Thomas, T.R. and Love, G.R., *Can. J. Phys.*, **30**, 577 (1952).
18. Spencer, H.M., *J. Chem. Phys.*, **14**, 729 (1946).
19. Evans, J.C. and Bernstein, H.J., *Can. J. Chem.*, **34**, 1083 (1956).
20. Miller, F.A. and Bauman, R.P., *J. Chem. Phys.*, **22**, 1544 (1954).
21. Wagner, J., *Z. Phys. Chem. B*, **45**, 69 (1939).
22. Lindeman, L.P. and Wilson, M.K., *J. Chem. Phys.*, **24**, 242 (1956).
23. Anderson, T.F., Lassettre, E.N. and Yost, D.M., *J. Chem. Phys.*, **4**, 703 (1936).